Detecting Small Structural Changes in Metalloproteins by the Use of NMR Pseudocontact Shifts

Marco Allegrozzi,[a] Ivano Bertini,*[a,b] Sung-Nak Choi,[c] Yong-Min Lee,[a] and Claudio Luchinat[a,d]

Keywords: Metalloproteins / Pseudocontact shifts / Lanthanides / Protein structures / Temperature-dependence / Magnetic susceptibility

The potential use of pseudocontact shifts (PCS) for detecting small structural changes that may occur in a protein in aqueous solution as a function of temperature is demonstrated on lanthanide-substituted calbindin D_{9k}. The protein is a dicalcium protein in which one of the calcium ions can be selectively substituted by lanthanides. The solution structure of the protein had been previously solved at 300 K. New sets of PCS that could readily be obtained at 280 and 310 K from ^{1}H-^{15}N HSQC experiments, together with the other constraints used for the 300 K structure, were used to recalculate the solution structure at the new temperatures, since the new solution structures are consistent with different sets of PCS constraints *and* a single NOE/dihedral angle set of constraints. Temperature-dependent PCS data were collected and analyzed for as many as eleven different paramagnetic lanthanides, but the relevant structural information could already be obtained by using data from only one [erbium(III)] derivative. It is found that small structural changes occur preferentially in nonhelical regions of the protein, i.e. the N- and C-terminal ends, in the linker region between the two helix-loop-helix motifs, as well as at the metal binding loops. This research shows that PCS are most sensitive to small structural rearrangements that may be within the tolerance of the NOE constraints, and can be safely used to monitor changes that would not be detectable by NOE and dihedral angle measurements. From the newly obtained structures, the parameters describing the metal magnetic susceptibility tensors at the different temperatures can be obtained, which represent a further source of information.

Introduction

Solution structures of proteins by NMR spectroscopy are often more cumbersome to obtain than solid state X-ray structures, and are often less resolved. However, the availability of structural information in solution is precious because the protein is closer to its native state and because dynamic information can be extracted from NMR spectroscopic parameters. Another advantage of NMR spectroscopy as a structural tool that is not often appreciated is that small structural changes, for instance those induced by denaturants at sub-denaturing conditions, by interactions with small chemical compounds or with other biomolecules, by pH changes or temperature changes, may be observed in favorable cases, while these changes may not be accessible under the conditions of crystallization. However, the most important class of NMR structural constraints, i.e. NOEs, can be safely used in a semi-quantitative way only, and small structural changes may escape detection. Paramagnetism-based constraints, such as the pseudocontact shifts (PCS)[1−3] that originate from the presence of a paramagnetic metal ion possessing magnetic susceptibility anisotropy, are more promising in this respect. This is due to the favorable functional form of the constraint, which involves both the metal-nucleus distance and the angular coordinates of the nucleus with respect to the principal axes of the magnetic susceptibility tensor, χ [Equation (1)][1,2,4]

$$\delta_i^{pc} = \frac{1}{12\pi r_i^3}\left[\Delta\chi_{ax}\left(3\cos^2\theta - 1\right) + \frac{3}{2}\Delta\chi_{rh}\left(\sin^2\theta\cos 2\Omega\right)\right] \quad (1)$$

[a] Magnetic Resonance Center (CERM), University of Florence
Via L. Sacconi, 6, 50019 Sesto Fiorentino, Italy
Fax: (internat.) +39-055/457-4271
E-mail: bertini@cerm.unifi.it
lee@cerm.unifi.it
allegrozzi@cerm.unifi.it
[b] Department of Chemistry, University of Florence
Via della Lastruccia, 5, 50019 Sesto Fiorentino, Italy
[c] Department of Chemistry, Pusan National University
Kumjeong-Ku, Pusan 609−735, Korea
E-mail: sunachoi@pusan.ac.kr
[d] Department of Agricultural Biotechnology, University of Florence
P. le delle Cascine, 24, 50144 Sesto Fiorentino, Italy
E-mail: luchinat@cerm.unifi.it
Supporting information for this article is available on the WWW under http://www.eurjic.com or from the author.

where $\Delta\chi_{ax}$ and $\Delta\chi_{rh}$ are the axial and the rhombic anisotropies of the magnetic susceptibility tensor, and r_i, θ and Ω are the polar coordinates of the nucleus *i*. Metalloproteins are ideal systems to measure PCS on nuclei around the metal ion (by taking care to avoid nuclei with contact shifts).

In this work we investigate the possibility of detecting small structural changes that may occur as a function of temperature in a suitable metalloprotein, for example the calcium-binding protein calbindin D_{9k}. The protein has two helix-loop-helix motifs, called EF-hands, joined by a linker region made more flexible by a Pro-Met (P43M) mutation. Each of the two loops hosts a calcium ion. The first EF-hand, the so called ''pseudo EF-hand'', consists of 14 residues and binds calcium by using four backbone carbonyl oxygen atoms and one side-chain carboxylic group, whereas the second EF-hand, the common EF-hand, consists of 12 residues and binds calcium by using one backbone carbonyl oxygen and four side-chain carboxylic groups. Both solution[5−7] and X-ray[8] structures of the protein are available, as well as mobility studies in solution.[9] We exploit the fact that lanthanide ions can be selectively substituted for calcium in the second calcium binding site, and in so doing generate pseudocontact shifts.[7,10,11] Indeed, the solution structure has been solved using the PCS constraints of the peptide NH nuclei, induced by as many as 11 different lanthanides.[7] Therefore, this seemed to us an ideal system to test the sensitivity of PCS towards minor temperature-dependent structural changes. Of course it is assumed (and verified a posteriori) that the structure of all of the lanthanide derivatives is the same.

In this approach two distinct types of phenomena are to be looked for: i) structural changes, occurring anywhere in the protein, causing a change in the polar coordinates of some nuclei with respect to the metal-centered tensor frame, and consequently changing their PCS values; ii) intrinsic (structure-independent) temperature-dependence of the magnetic susceptibility tensor parameters which alter the PCS values of all protein atoms.

Results and Discussion

Structure Calculations at the Three Temperatures

Thirteen sets of ^{15}N-^{1}H HSQC shifts at 280 and 310 K for the peptide ^{15}N-^{1}H nuclei of lanthanide-substituted calbindin D_{9k} have been collected, and added to the existing 300 K data.[7] The two sets of data for the diamagnetic derivatives CaLaCb and CaLuCb were used as a blank for the other 11 paramagnetic sets of data as previously reported.[7] The resulting PCS values are 966 PCS at 280 K and 1028 PCS at 310 K. These data, together with the previously determined 1097 PCS at 300 K,[7] are reported as supplementary material (Table S1). The number of observed ^{1}H-^{15}N HSQC cross-peaks at 310 K are almost the same as those at 300 K, however, there are fewer ^{1}H-^{15}N HSQC cross-peaks at 280 K than at 300 or 310 K, probably due to the increased paramagnetism at lower temperatures.

From the 11 sets of data at each temperature and from the existing solution structure at 300 K,[7] initial estimates of the magnetic susceptibility tensor anisotropies and orientations were obtained using the program FANTASIA.[12] Separate structure calculations were then performed using the program PSEUDYANA,[13] the PCS constraints at either 280 or 310 K, and all the NOEs and other diamagnetic constraints previously collected at 300 K.[14] The rationale behind this procedure is that as long as structure alterations with respect to the 300 K structure are modest, the expected violations of the NOE constraints are within the tolerance level, and this can be verified a posteriori.

After an initial family of structures was obtained at each temperature, the values of the tensors were recalculated using FANTASIA,[12] and PSEUDYANA[13] runs were repeated until convergence was obtained. Calculations were also repeated for the 300 K data, which obviously gave the same family and the same tensors as obtained previously, within the uncertainty margin. The structures at 280 and 310 K showed modest differences (which were outside the uncertainty margin) from the one at 300 K, as well as from one another. A quality factor[7,15] was determined which showed that the agreement between calculated and experimental PCS is good at all three temperatures. The global RMSD values are reported in Table 1, together with the quality factors and target functions at the three temperatures. The latter were somewhat higher than those of the structure at 300 K. This finding is important because it provides an a posteriori validation of the use of NOE constraints at one temperature as structural constraints for a different temperature. This was not completely unexpected, however, as NOE constraints are applied in the form of upper distance limits, and the structural variations are probably within their tolerance level. The final values of the five parameters for the 11 paramagnetic derivatives, together with their errors evaluated through a Monte Carlo analysis,[7] at the three temperatures are presented in Table 2. They will be discussed further, in the context of the analysis of possible structural alterations at the binding site.

Analysis of the Structural Differences

As suggested by the RMSD values in Table 1, structural differences outside the uncertainty seem to arise from changes in temperature for calbindin D_{9k}. A more detailed analysis of the nature and significance of these differences can be attempted by examining the RMSD per residue between the structures at the three temperatures. Figure 1 illustrates the pairwise RMSD per residue between each pair of structures, both referred to the backbone and to all the heavy atoms. It is clear that in several places of the sequence the agreement is significantly poorer than that within each family. This is particularly apparent in the N- and C- terminal parts, in the metal binding loops, as well as in the region of the linker between the two helix-loop-helix motifs, i.e. in all nonhelical parts of the structure. Although the nonhelical regions are those with intrinsically larger RMSD within each family, the RMSD between the families are well above the sum of the RMSD within each family in these

Table 1. Global RMSD, together with the target functions and quality factors for the families of structures at the three temperatures, and RMSD between mean structures at the two temperatures

	RMSD (bb) (2−74)		RMSD (heavy) (2−74)		Tf	Q^{pc}
	from the average	pairwise	from the average	pairwise		
280 K (30 structures)	0.32 ±0.07	0.44 ±0.10	0.79 ±0.08	1.10 ±0.11	4.2	0.14
300 K (30 structures)	0.31 ±0.07	0.43 ±0.10	0.80 ±0.07	1.11 ±0.10	1.9	0.16
310 K (30 structures)	0.34 ±0.08	0.47 ±0.11	0.81 ±0.07	1.14 ±0.10	2.6	0.16
Between 280 K and 300 K	0.80 ± 0.10		1.20 ± 0.15		–	–
Between 280 K and 310 K	0.90 ± 0.10		1.18 ± 0.11		–	–
Between 300 K and 310 K	0.88 ± 0.10		1.19 ± 0.15		–	–

Table 2. Magnetic susceptibility tensor anisotropies, $\Delta\chi_{ax}$ and $\Delta\chi_{rh}$, calculated from the solution structure at each temperature

Metal	$\Delta\chi_{ax}$ (10^{-32} m^3)[a]			$\Delta\chi_{rh}$ (10^{-32} m^3)[a]		
	310 K	300 K	280 K	310 K	300 K	280 K
Ce	1.81 ± 0.10	1.91 ± 0.13	2.34 ± 0.11	0.87 ± 0.11	0.76 ± 0.13	0.89 ± 0.14
Pr	2.69 ± 0.07	3.37 ± 0.29	3.94 ± 0.22	2.16 ± 0.07	2.31 ± 0.14	2.56 ± 0.17
Nd	1.38 ± 0.12	1.53 ± 0.14	2.22 ± 0.12	0.54 ± 0.16	0.38 ± 0.13	0.39 ± 0.22
Sm	0.19 ± 0.12	0.36 ± 0.11	0.19 ± 0.07	0.16 ± 0.06	0.12 ± 0.05	0.07 ± 0.05
Eu	1.84 ± 0.15	2.44 ± 0.17	1.78 ± 0.27	0.71 ± 0.27	1.50 ± 0.29	0.86 ± 0.43
Tb	38.2 ± 3.6	42.3 ± 3.3	52.7 ± 2.6	12.8 ± 2.1	10.0 ± 2.1	11.8 ± 1.5
Dy	34.8 ± 0.7	35.7 ± 2.1	36.5 ± 2.7	20.7 ± 0.5	21.2 ± 2.0	25.3 ± 2.1
Ho	17.1 ± 0.7	20.0 ± 0.8	20.9 ± 1.0	6.85 ± 0.95	4.68 ± 0.65	6.27 ± 0.89
Er	11.4 ± 0.2	11.6 ± 0.2	14.2 ± 0.3	5.38 ± 0.68	7.32 ± 0.40	10.2 ± 0.7
Tm	26.5 ± 0.9	27.4 ± 0.9	30.4 ± 0.6	11.3 ± 1.2	12.2 ± 0.9	14.2 ± 1.6
Yb	7.14 ± 0.51	8.03 ± 0.37	9.66 ± 0.31	3.63 ± 0.45	4.44 ± 0.50	5.05 ± 0.73

[a] The uncertainties reported correspond to the sum of the standard deviation of the tensor parameters resulting from either the fit of the individual conformers of the family, or fitting partial data sets in which 30% of the input data were randomly deleted according to a MonteCarlo analysis.

regions (Figure 1). In particular, noticeable temperature changes are shown by the φ and ψ angles of the residues in the first loop (residues 17, 18, 21, 22 and 23), in the linker and beginning of the third helix (residues 36−48) and in the second loop (residues 56−62). Furthermore, the orientations of the side-chain of residues Glu 17, Gln 22, Lys 41 and Asn 56 are somewhat different. However, the overall quality of the three structures based on Ramachandran plots[16] is very similar (about 89% of residues in most favored regions and 11% in additionally allowed regions at all temperatures). Interestingly, residues 17, 41 and 56 all precede a glycine in the sequence. The lower conformational barrier of glycine could be responsible for the temperature sensitivity of the preceding residues. The fact that significant differences among the three families are observed, despite the use of a single set of NOEs, suggests that the actual differences may be even larger. Figure 2 summarizes the regions of the protein where temperature-dependent structural changes are observed.

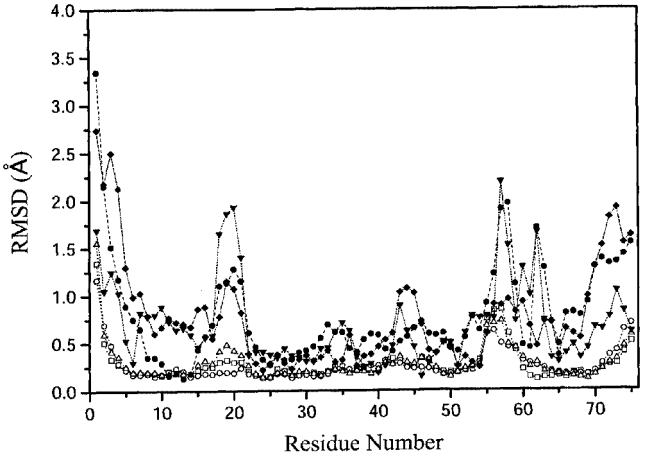

Figure 1. RMSD per residue within each family of structures at 280 K (□), 300 K (○) and 310 K (△), and between mean structures at the two temperatures, 280 K-300 K (▼), 280 K−310 K (◆) and 300 K−310 K (●)

In order to test whether the present results could still be obtained in systems where only one paramagnetic derivative is available, the solution structures at three temperatures were also calculated using the PCS of only the Er^{3+} derivative (chosen among the eleven lanthanides because it provides a sufficiently high number of ^{15}N-^{1}H HSQC cross-peaks with nonnegligible PCS values). The pairwise RMSD values of each family at each of the three temperatures for the backbone are in the range 0.71−0.77 Å, while the RMSD between the different families of structures at the three temperatures are in the range 0.80−1.07 Å. Based on Ramachandran plots,[16] the overall quality of the structures from the Er^{3+} derivative is the same as that from 11 lanthanide derivatives. In all nonhelical parts of the three

Figure 2. Schematic representation of the solution structure of calbindin D_{9k}, highlighting the residues that undergo slight temperature-dependent structural changes (shaded in dark gray)

structures of the Er^{3+} derivative at different temperatures, the agreement is sizably poorer than that within each family. In particular, the φ and ψ angles of the residues in the first loop (residues 19−22), linker (residues 41−44) and second loop (residues 54−62) were affected by variations in temperature. These results are very similar to those obtained by making use of the PCS data for all eleven lanthanide derivatives, and therefore show: i) that the assumption that the structure is lanthanide-independent is verified, and ii) that the present approach may be of general applicability for any paramagnetic metalloprotein.

The significance of the observed temperature-related changes, at least in regions far from the paramagnetic center, should be further checked by going back to the original PCS data. This practice is common in the analysis of differences between solution structures, and originates from the fact that, due to the global nature of the simulated annealing procedure and the local nature of the structural changes, the best check to ascertain the significance of the latter is to relate them to local variations of the constraints. In the present case, the simple comparison of the PCS data at different temperatures for a particular residue or group of residues is not feasible, as: i) a temperature-dependent variation of the magnitude of the tensor parameters (and therefore of the PCS values) is theoretically expected, independent of structural variations, and ii) structural changes at the metal ion site would also alter the tensors, and therefore all the PCS, simultaneously. Therefore, a way of comparing the PCS values should be found that is independent of the tensor variations. A possibility is that of examining the *ratios* between the ^{15}N and ^{1}H PCS for a given NH group for each lanthanide. This ratio should be much less sensitive to tensor variations than to changes in orientation of the N−H vector with respect to either the M−N or M−H vectors.

Therefore, again assuming the same behavior for all lanthanides, a plot of ^{15}N chemical shifts versus ^{1}H chemical shifts of a given NH group for all lanthanides at the same temperature should be a straight line. The slope, which depends on the third power of the ratio between the M−N and M−H distances, is expected not to exceed the range 0.77−1.3 for all NH groups that are farther than 12 Å from the metal.

In the absence of temperature-dependent structural variations, such straight lines for each temperature should be identical, whereas variations in the slopes should indicate a structural change. Examples of such plots are reported in Figure 3. The slopes for Ser 2, Phe 36 and Gly 42 indicate some temperature-dependent changes, whereas Leu 32 and Leu 69 are examples that exhibit structural invariance. From this qualitative analysis evidence is provided for temperature-dependent structural changes for residues Ser 2, Gly 18, Phe 36, Gly 42, Leu 46, Asp 47, Glu 48 and Gly 57, all in nonhelical regions. Despite the fact that the number of residues does not fully correspond to those which show variations in the structure, they still support the hypothesis that indeed the loops and linker undergo temperature-dependent changes. In any case, the structures at the three temperatures reliably show differences in about 25 residues, seven of which are confirmed spectroscopically.

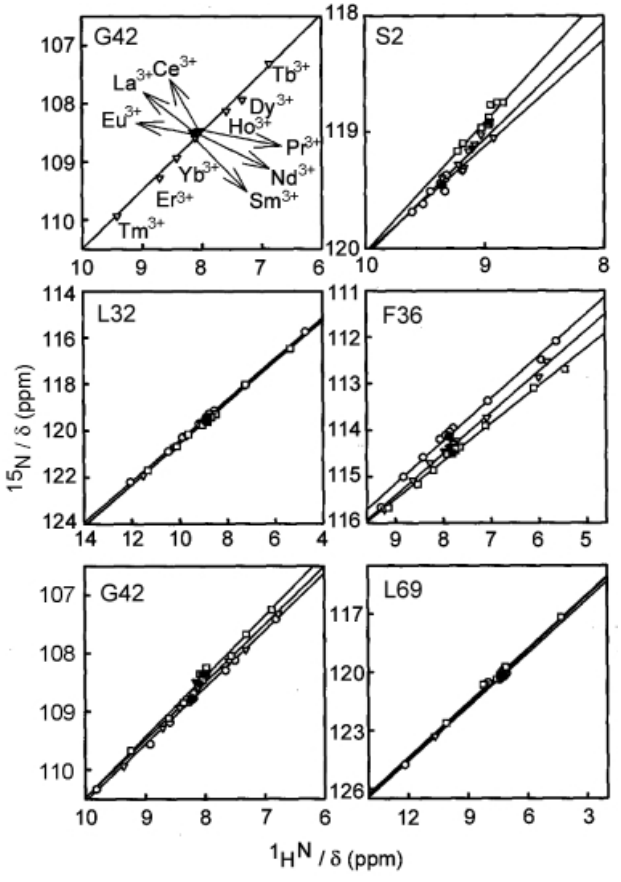

Figure 3. Observed ^{15}N versus ^{1}H chemical shifts of the G42 NH moiety (upper left) with all lanthanide ions at 300 K (▽) (diamagnetic CaLaCb values as filled symbols); analogous plots for selected residues at 280 K (○), 300 K (▽), and 310 K (□) are also shown

Temperature-Dependence of the Tensor Parameters

It is worth examining the temperature-dependence of the $\Delta\chi_{ax}$ and $\Delta\chi_{rh}$ parameters. Theory predicts that these parameters should experience a temperature dependence that is proportional to the temperature dependence of the overall magnetic susceptibility. The latter is expected to have a T^{-2} dependence, with modest positive or negative corrections from a T^{-3} term arising from the thermal population of the excited electronic states.[17–19] The $\Delta\chi_{ax}$ values for the 11 lanthanides as a function of T^{-2} are reported in Figure 4. Most lanthanides show a monotonous change with temperature, with the exception of samarium(III) and europium(III). The behavior of the latter two ions is unexpected. However, the collection of a number of experimental data at different temperatures to address this point is beyond the scope of this paper. Although a quantitative assessment of the slopes is difficult to make, some lanthanides clearly show a more marked temperature dependence [e.g. terbium(III)] and some a less marked one [e.g. dysprosium(III)]. Inspection of Table 2 reveals that some modest, but consistent, changes in the angular parameters are also observed for all lanthanides. Figure 5 illustrates such changes in the form of plots of θ vs. φ, where θ and φ are the angles defining the orientation of the principal axes of the χ tensor with respect to a fixed reference frame. The changes are on average between 5 and 10 degrees, with the largest (almost 20 degrees) being observed for the holmium(III) derivative. These changes are of the same order as the uncertainties; however they are in all cases monotonous with temperature i.e. they have a systematic character that cannot be explained by random errors. In summary, changes both in the magnitude of the susceptibility anisotropy parameters and in the principal axes orientations are detected over the temperature range investigated. The changes in axes orientation, in particular, suggest that population of excited states involving different *f*-orbitals may occur. Overall, the present analysis shows that possible structural or electronic changes at the metal site can be recognized as such and do not prevent detection of small temperature-dependent structural changes in the protein part of paramagnetic metalloproteins when using PCS.

The possibility that the present analysis may be hampered by some kind of circular argument could be considered. However, it is easy to show that the ratios of the PCS values for the ^{15}N and ^{1}H nuclei of a peptide NH moiety are much less sensitive to the orientation of the tensor axes than they are to changes in the orientations of the NH vectors. Furthermore, the tensor parameters are barely sensitive to structural variations that occur far from the metal center and that essentially compensate each other. Sample calculations show that random variations (up to ±40°) of ten different NH vector orientations (i.e. larger structural changes than those observed here) change the magnetic anisotropy parameters of the various lanthanide ions by much less (typically less than 1%) than the changes due to temperature. In another set of sample calculations, variations of ±5° in the tensor orientation for the lanthanide ions with the largest magnetic susceptibility anisotropy change the δ_N/δ_H ratios of the NH groups with the largest pseudocontact shift by less than 4%, i.e., much less than the observed changes in the slopes that have been considered meaningful indications of true structural changes.

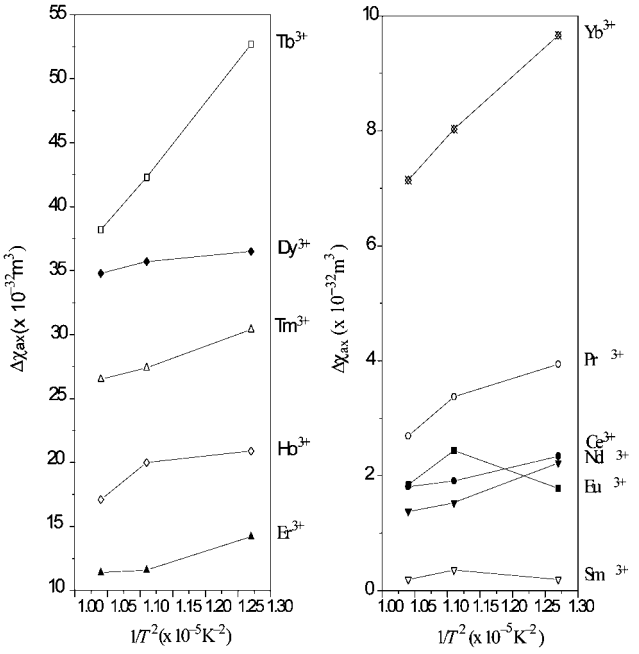

Figure 4. Plot of experimental $\Delta\chi_{ax}$ values vs. $1/T^2$ for all lanthanide ions

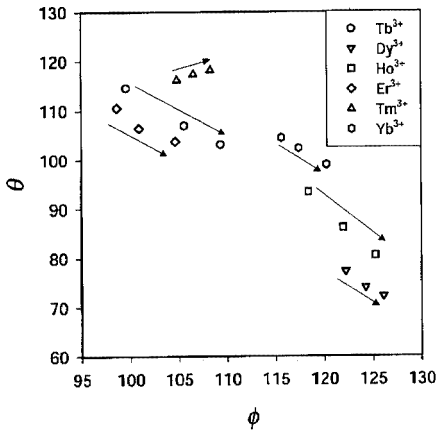

Figure 5. Temperature dependence of the θ and φ values of the principal axis of the χ tensor for the second half of the lanthanide series; the reference system is arbitrary and fixed to the molecular frame; the arrows indicate increasing temperature

Concluding Remarks

The power of PCS in determining the solution structure is proved by the finding that minor changes of PCS, for example with temperature, can be used to relate them to small structural changes, by solving the solution structure with a common set of NOEs and appropriate PCS. This is

shown through lanthanide substitution of a calcium binding protein, calbindin D_{9k}. This finding is qualitative, but is definitively confirmed by the analysis of the $^{15}N/^{1}H$ PCS ratios for NH moieties. If no temperature-dependent change occurs in the NH orientation, the above ratio is constant, even if modest temperature-dependent changes in the metal magnetic susceptibility occur. From the different solution structures, the magnetic susceptibility anisotropies at different temperatures are obtained which are additional and precious pieces of information that may be further analyzed.

Experimental Section

Materials and Methods

Sample Preparation: Protein expression and purification of the ^{15}N-enriched dicalcium form of bovine calbindin D_{9k} (P43M mutant) was performed as reported previously.[20−23] NMR samples were prepared by dissolving the lyophilized protein in 500 μL of 90% H_2O/10% D_2O to give final 2.0 mM protein solutions. The pH was adjusted to 6.0 by means of 0.1 M NaOH or 0.1 M HCl. Lanthanide-containing calbindin D_{9k} (hereafter CaLnCb) samples were obtained by titrating the dicalcium form with 0.02 M solutions of analytical grade $LnCl_3$ (Sigma, Aldrich), up to one equivalent.[7,24] Titrations were followed by 2D ^{1}H-^{15}N HSQC spectroscopy. The samples were kept at 4 °C between measurements.

NMR Spectroscopy: NMR spectra were acquired on Bruker AVANCE 800 and 400 spectrometers operating at 800.13 and 400.13 MHz, respectively. The residual water signal was suppressed by either presaturation during both the relaxation delay and mixing time, or by gradient-tailored excitation (WATERGATE).[25] The spectra were calibrated in the proton dimension at different temperatures according to the empirical relationship[26] $\delta_{HOD} = (-0.012 \times T + 5.11)$ ppm, where T is the temperature in °C. ^{1}H-^{15}N HSQC[27] spectra were recorded for all lanthanide derivatives at 280, 300 and 310 K using a spectral width of 16 ppm and 36 ppm in the ^{1}H and ^{15}N dimension, respectively. 512 increments, each with 1024 complex data points and 32 transients, were collected. The recycle delays were in the range between 0.5 s (CaTbCb) and 1.0 s (CaLaCb). All NMR spectroscopic data were processed with the Bruker XWINNMR software packages. The program XEASY was used for analysis of the 2D spectra.[28]

Computer Programs: The programs FANTASIA, PSEUDYANA are available at http://www.postgenomicNMR.net

Determination of PCS and Simultaneous Refinement of Magnetic Tensor Anisotropies and Solution Structure: Pseudocontact shifts for each paramagnetic lanthanide derivative at 280, 300 and 310 K were calculated by subtracting the shifts of either the CaLaCb or the CaLuCb diamagnetic protein. The pseudocontact shifts at 300 K have been taken from previous work without modification.[7] The variations in pseudocontact shifts for each lanthanide derivative at 280 and 310 K were directly calculated as the differences from the chemical shifts of each lanthanide derivative at 300 K.
The magnetic susceptibility tensor anisotropies for each lanthanide, $\Delta\chi_{ax}$ and $\Delta\chi_{rh}$, were obtained by simultaneously fitting all the PCS values to a family of 30 conformers obtained from solution structure calculations through Equation (1), and the error estimated through a MonteCarlo analysis.[7] These calculations were accomplished with the program FANTASIA.[12] Solution structure calculations at each temperature were performed using all diamagnetic constraints (NOEs, van der Waals) at 300 K and PCS constraints at each temperature. These diamagnetic constraints have been taken from previous work.[14] These amounted to 1793 meaningful NOEs, 191 dihedral angles, 15 hydrogen bonds and 26 T_1.
The quality factor for PCS was defined as:[7,15]

$$Q^{ax} = \frac{\sqrt{\sum_i \left(\delta_i^{obs} - \delta_i^{calc}\right)^2}}{\sqrt{\sum_i \left(\delta_i^{obs}\right)^2}} \qquad (2)$$

where δ_i^{obs} is the i-th experimental PCS value measured, δ_i^{calcd} is the corresponding calculated PCS value, and the summations span all experimental PCS.

Supporting Information Available: A table reporting the PCS values used in the solution structure calculations at three temperatures for all lanthanide derivatives (PDF); see also footnote on the first page of this article.

Acknowledgments

This research has been financially supported under the RTD project (Contracts QLG2-CT-1999−01003 for FIND structure and HPR1-1999-CT-50006 for Transient NMR). This work also has been supported partly by MIUR, ex 40%, and CNR (Contracts 97.01133.49, 98.01789.CT03, and 99.00393.49). Financial support of the EU through Contract No.: QLG2-CT-1999-01003 to Y.-M.L. is gratefully acknowledged.

[1] H. M. Mc Connell, R. E. Robertson, *J. Chem. Phys.* **1958**, *29*, 1361−1365.
[2] R. J. Kurland, B. R. McGarvey, *J. Magn. Reson.* **1970**, *2*, 286−301.
[3] I. Bertini, C. Luchinat, G. Parigi, *Solution NMR of Paramagnetic Molecules*, Amsterdam, Elsevier, **2001**.
[4] L. Banci, I. Bertini, K. L. Bren, M. A. Cremonini, H. B. Gray, C. Luchinat, P. Turano, *J. Biol. Inorg. Chem.* **1996**, *1*, 117−126.
[5] J. Kordel, N. J. Skelton, W. J. Chazin, *J. Mol. Biol.* **1993**, *231*, 711−734.
[6] D. M. E. Szebenyi, K. J. Moffat, *J. Biol. Chem.* **1986**, *261*, 8761−8777.
[7] I. Bertini, M. B. L. Janik, Y.-M. Lee, C. Luchinat, A. Rosato, *J. Am. Chem. Soc.* **2001**, *123*, 4181−4188.
[8] L. A. Svensson, E. Thulin, S. Forsén, *J. Mol. Biol.* **1992**, *223*, 601−606.
[9] I. Bertini, C. J. Carrano, C. Luchinat, M. Piccioli, L. Poggi, *Biochemistry* **2002**, *41*, 5104−5111.
[10] H. J. Vogel, T. Drakenberg, S. Forsén, J. D. O′Neil, T. Hofmann, *Biochemistry* **1985**, *24*, 3870−3876.
[11] M. Akke, S. Forsén, W. J. Chazin, *J. Mol. Biol.* **1991**, *220*, 173−189.
[12] L. Banci, I. Bertini, G. Gori Savellini, A. Romagnoli, P. Turano, M. A. Cremonini, C. Luchinat, H. B. Gray, *Proteins Struct. Funct. Genet.* **1997**, *29*, 68−76.
[13] L. Banci, I. Bertini, M. A. Cremonini, G. Gori Savellini, C. Luchinat, K. Wüthrich, P. Güntert, *J. Biomol. NMR* **1998**, *12*, 553−557.
[14] I. Bertini, A. Donaire, B. Jimenez, C. Luchinat, G. Parigi, M. Piccioli, L. Poggi, *J. Biomol. NMR* **2001**, *21*, 85−98.
[15] G. Cornilescu, J. Marquardt, M. Ottiger, A. Bax, *J. Am. Chem. Soc.* **1998**, *120*, 6836−6837.
[16] R. A. Laskowski, M. W. MacArthur, D. S. Moss, J. M. Thornton, *J. Appl. Crystallogr.* **1993**, *26*, 283−297.

[17] B. Bleaney, *J. Magn. Reson.* **1972**, *8*, 91−100.
[18] W. D. Horrocks, Jr., *J. Magn. Reson.* **1977**, *26*, 333−339.
[19] B. R. McGarvey, *J. Magn. Reson.* **1979**, *33*, 445−455.
[20] P. Brodin, T. Grundstrom, T. Hofmann, T. Drakenberg, E. Thulin, S. Forsén, *Biochemistry* **1986**, *25*, 5371−5377.
[21] C. Johansson, P. Brodin, T. Grundstrom, E. Thulin, S. Forsén, T. Drakenberg, *Eur. J. Biochem.* **1990**, *187*, 455−460.
[22] A. Malmendal, G. Carlström, C. Hambraeus, T. Drakenberg, S. Forsén, M. Akke, *Biochemistry* **1998**, *37*, 2586−2595.
[23] W. J. Chazin, J. Kördel, T. Drakenberg, E. Thulin, P. Brodin, T. Grundstrom, S. Forsén, *Proc. Natl. Acad. Sci. U. S. A.* **1989**, *86*, 2195−2198.
[24] M. Allegrozzi, I. Bertini, M. B. L. Janik, Y.-M. Lee, G. Liu, C. Luchinat, *J. Am. Chem. Soc.* **2000**, *122*, 4154−4161.
[25] M. Piotto, V. Saudek, V. Sklenar, *J. Biomol. NMR* **1992**, *2*, 661−666.
[26] I. Bertini, S. Ciurli, A. Dikiy, C. Luchinat, *J. Am. Chem. Soc.* **1993**, *115*, 12020−12028.
[27] G. Bodenhausen, D. J. Ruben, *Chem. Phys. Lett.* **1980**, *69*, 185−188.
[28] C. Eccles, P. Güntert, M. Billeter, K. Wüthrich, *J. Biomol. NMR* **1991**, *1*, 111−130.

Received November 28, 2001
[I01483]